

## Model Compounds Study on the Network Structure of Polybenzoxazines

Ho-Dong Kim and Hatsuo Ishida\*

*Department of Macromolecular Science and Engineering, Case Western Reserve University, Cleveland, Ohio 44106**Received February 13, 2003*

**ABSTRACT:** The FT-IR and  $^1\text{H}$  NMR spectra of model dimers, having different molecular sizes and  $\text{p}K_{\text{a}}$ , are investigated in order to understand the differences in the hydrogen-bonded network structures of polybenzoxazines. The correlation between the  $-\text{OH}\cdots\text{N}$  intramolecular hydrogen-bonding interaction and benzoxazine functional groups in the asymmetric dimers is investigated by  $^1\text{H}$  NMR spectra. While the FT-IR spectra of the model dimers indicate that the nature of hydrogen bonding is closely related to the basicity of the amine constituent, the spectra of the corresponding polymers suggest the existence of different hydrogen-bonding interactions. The existence of phenolic linkage formation and the stability of the Mannich base structure during polymerization are investigated by a dimerization reaction. It is demonstrated that benzoxazines based upon extremely bulky amines do not develop desirable properties due to the extensive degradation process.

## Introduction

It is well-known that hydrogen bonds play an important role in the wide range of material properties, and therefore, many studies have been actively done in this area.<sup>1–3</sup> Recently, a novel class of phenolic resins, polybenzoxazines, which can overcome many shortcomings associated with traditional phenolic resins, has been synthesized and characterized by Ishida et al.<sup>4–7</sup> Since the wide variety of benzoxazine monomers can be easily obtained by changing the primary amine component in Mannich condensation, they are of great interest for commercial applications. Furthermore, these resins have many excellent properties, which easily surpass the phenolic resins, such as excellent mechanical properties,<sup>4,5</sup> high char yield,<sup>5</sup> near zero volumetric shrinkage/expansion upon polymerization,<sup>6</sup> low water absorption<sup>4</sup> (despite the large amount of hydroxyl groups in the backbone structure), excellent resistance to chemicals<sup>8</sup> and UV light,<sup>9</sup> and amazingly high  $T_g$ ,<sup>10</sup> even with rather low cross-link density. A possible explanation for these unusual properties is the formation of extensive hydrogen-bonding networks.<sup>11</sup>

Consequently, the effort to understand the fundamental nature of the hydrogen-bonding structure of polybenzoxazines has been a recent focus of this laboratory.<sup>6,8,12–14</sup> To overcome the instrumental limitation in studying thermoset polymer structures and to better investigate the complex relation between several hydrogen-bonding species, a series of model compounds were synthesized.<sup>12,13</sup> Investigating the FT-IR spectra and X-ray crystallographic structure for *N,N*-bis(3,5-dimethyl-2-hydroxybenzyl)methylamine, Dunkers et al.<sup>12</sup> proposed a hydrogen-bonding scheme involving both  $\text{OH}\cdots\text{O}$  intermolecular and intramolecular hydrogen bonding as well as  $\text{OH}\cdots\text{N}$  intramolecular hydrogen bonding. The more precise FT-IR band assignments for each hydrogen species in benzoxazine model compounds were reported by Kim et al.<sup>13</sup> by comparing the spectra for simplified asymmetric dimers and an aromatic amine-based model dimer. Also, they proposed a difference in network structure between aliphatic amine-based polybenzoxazines and aromatic amine-based polybenzoxazines. One possibility for this difference, the

intramolecular hydrogen-bonding interactions, was studied by Ishida et al.<sup>6</sup> using molecular modeling of benzoxazine dimers based on different amine functional groups. They reported that the compactness of a network structure is related to both the basicity and bulkiness of the functional amines.

However, the previous studies were based on the assumption that the bulk of monomer is converted to polymer upon curing, resulting in a pure polybenzoxazine structure which solely consisted of Mannich bridges between phenolic groups. Moreover, despite the important effect of the amine substituents on hydrogen bonding, research has been conducted only on a few simple dimer molecules.<sup>6,12</sup> A more detailed study of the network structures in the polymers using model dimers will allow for a better explanation of the behavior of the polymers. Therefore, this paper will investigate the effect of amine functional groups on the hydrogen bonding and network structure using a series of model dimers and polymers.

## Experimental Section

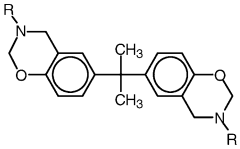
All chemicals were obtained from Aldrich with high purity (above 98%), except for formaldehyde (Fisher, 37% in  $\text{H}_2\text{O}$ ), and used as received.

**Synthesis of Polybenzoxazine Monomers and Polymers.** Benzoxazine monomers, based on bisphenol A, were synthesized and purified according to the procedure of Ning and Ishida<sup>7</sup> or Ishida.<sup>15</sup> These benzoxazine monomers were polymerized without added initiator or catalyst according to the method reported in a previous paper.<sup>8</sup> The monomers used are summarized in Table 1, and the generalized polymer structure is shown in Scheme 1.

**Synthesis of Symmetric Dimers.** The symmetric model dimers for polybenzoxazines were synthesized according to a previous study using 2,4-dimethylphenol, formaldehyde, and primary amines.<sup>16</sup> All products except for the aniline dimer were recrystallized three times in hexane. The aniline dimer was recrystallized from hexane and subsequently purified by column chromatography with silica gel using hexane/methylene chloride (20:1) as the eluent. The resulting dimers are summarized in Table 2, and the dimer formation reaction is shown in Scheme 2.

**Synthesis of Asymmetric Dimers.** The asymmetric model dimers based on different primary amines (Table 3), which have only one hydroxyl group in the structure, were synthe-

Table 1. Polybenzoxazine Monomers



| Abbreviations | R  | IUPAC chemical names   |
|---------------|--|--|
| 1a (BA-m)     | -CH <sub>3</sub>                                 | 2,2-bis(3,4-dihydro-3-methyl-2H-1,3-benzoxazine)propane                  |
| 1b (BA-e)     | -CH <sub>2</sub> CH <sub>3</sub>                 | 2,2-bis(3,4-dihydro-3-ethyl-2H-1,3-benzoxazine)propane                   |
| 1c (BA-p)     | -(CH <sub>2</sub> ) <sub>2</sub> CH <sub>3</sub> | 2,2-bis(3,4-dihydro-3- <i>n</i> -propyl-2H-1,3-benzoxazine)propane       |
| 1d (BA-nb)    | -(CH <sub>2</sub> ) <sub>3</sub> CH <sub>3</sub> | 2,2-bis(3,4-dihydro-3- <i>n</i> -butyl-2H-1,3-benzoxazine)propane        |
| 1e (BA-tb)    | -C(CH <sub>3</sub> ) <sub>3</sub>                | 2,2-bis(3,4-dihydro-3- <i>tert</i> -butyl-2H-1,3-benzoxazine)propane     |
| 1f (BA-c)     | -C <sub>6</sub> H <sub>11</sub>                  | 2,2-bis(3,4-dihydro-3-cyclohexyl-2H-1,3-benzoxazine)propane              |
| 1g (BA-Bz)    | -CH <sub>2</sub> Ar                              | 2,2-bis(3,4-dihydro-3-benzyl-2H-1,3-benzoxazine)propane                  |
| 1h (BA-a)     | -C <sub>6</sub> H <sub>5</sub>                   | 2,2-bis(3,4-dihydro-3-phenyl-2H-1,3-benzoxazine)propane                  |
| 1i (BA-fa)    | -C <sub>6</sub> H <sub>4</sub> F                 | 2,2-bis(3,4-dihydro-3- <i>o</i> -fluorophenyl-2H-1,3-benzoxazine)propane |

Scheme 1. Ring-Opening Polymerization of Bifunctional Benzoxazine Monomer

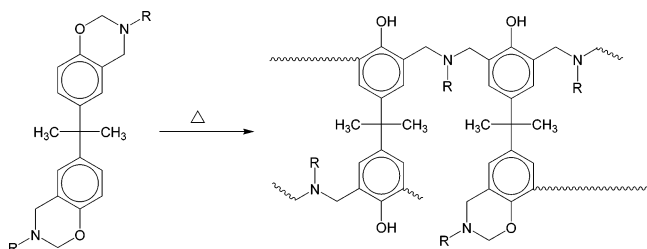
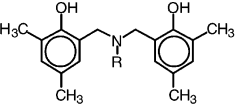
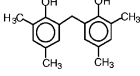


Table 2. Symmetric Model Dimers



| Abbreviations         | R   | IUPAC chemical names   |
|-----------------------|---|--|
| 2a (Methyl-dimer)     | -CH <sub>3</sub>  | N,N-bis(3,5-dimethyl-2-hydroxybenzyl)methylamine             |
| 2b (Ethyl-dimer)      | -CH <sub>2</sub> CH <sub>3</sub>  | N,N-bis(3,5-dimethyl-2-hydroxybenzyl)ethylamine              |
| 2c (Propyl-dimer)     | -(CH <sub>2</sub> ) <sub>2</sub> CH <sub>3</sub>                                    | N,N-bis(3,5-dimethyl-2-hydroxybenzyl)- <i>n</i> -propylamine |
| 2d (Cyclohexyl-dimer) | -C <sub>6</sub> H <sub>11</sub>   | N,N-bis(3,5-dimethyl-2-hydroxybenzyl)cyclohexylamine         |
| 2e (Aniline-dimer)    | -C <sub>6</sub> H <sub>5</sub>  | N,N-bis(3,5-dimethyl-2-hydroxybenzyl)aniline                 |
| 3 (Phenolic-dimer)    |  | bis(3,5-dimethyl-2-hydroxyphenyl)methane                     |

sized according to the previous study.<sup>13</sup> To synthesize the asymmetric methyl dimer, asymmetric ethyl dimer, asymmetric *tert*-butyl dimer, asymmetric aniline dimer, and the asymmetric benzylic dimer, stoichiometric mixtures of 2,4-dimethylphenol, paraformaldehyde, and the corresponding *N*-methylbenzylamine, *N*-ethylbenzylamine, *N*-*tert*-butylben-

Scheme 2. Formation of Model Dimers

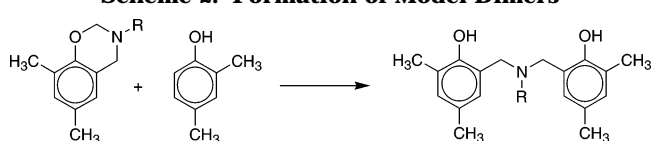
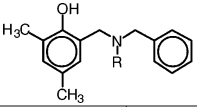
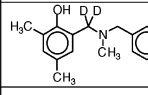


Table 3. Asymmetric Model Dimers I



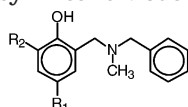
| Abbreviations                           | R   | IUPAC chemical names   |
|---|---|--|
| 4a (Asymmetric Methyl-dimer)            | -CH <sub>3</sub>  | N-benzyl-N-(3,5-dimethyl-2-hydroxybenzyl)methylamine                                   |
| 4b (Asymmetric deuterated Methyl-dimer) |  | N-benzyl-N-(3,5-dimethyl-2-hydroxybenzyl)- $\alpha,\alpha$ -d <sub>2</sub> methylamine |
| 4c (Asymmetric Ethyl-dimer)             | -CH <sub>2</sub> CH <sub>3</sub>  | N-benzyl-N-(3,5-dimethyl-2-hydroxybenzyl)ethylamine                                    |
| 4d (Asymmetric Propyl-dimer)            | -(CH <sub>2</sub> ) <sub>2</sub> CH <sub>3</sub>                                    | N-benzyl-N-(3,5-dimethyl-2-hydroxybenzyl)- <i>n</i> -propylamine                       |
| 4e (Asymmetric <i>t</i> -Butyl-dimer)   | -C(CH <sub>3</sub> ) <sub>3</sub>   | N-benzyl-N-(3,5-dimethyl-2-hydroxybenzyl)- <i>tert</i> -butylamine                     |
| 4f (Asymmetric Cyclohexyl-dimer)        | -C <sub>6</sub> H <sub>11</sub>   | N,N-bis(3,5-dimethyl-2-hydroxybenzyl)cyclohexylamine                                   |
| 4g (Asymmetric Benzylic-dimer)          | -CH <sub>2</sub> C <sub>6</sub> H <sub>5</sub>                                      | N-benzyl-N-(3,5-dimethyl-2-hydroxybenzyl)benzylamine                                   |
| 4h (Asymmetric Aniline-dimer)           | -C <sub>6</sub> H <sub>5</sub>  | N-benzyl-N-(3,5-dimethyl-2-hydroxybenzyl)aniline                                       |
| 4i (Asymmetric Fluoroaniline-dimer)     | -C <sub>6</sub> H <sub>4</sub> F  | N-benzyl-N-(3,5-dimethyl-2-hydroxybenzyl)- <i>o</i> -fluoroaniline                     |

zylamine, dibenzylamine, and *N*-phenylbenzylamine were reacted without solvent at 105 °C for 1 h. The products were then dissolved in chloroform, washed several times with distilled water, and dried over sodium sulfate. The residual products were purified by column chromatography with silica gel using various solvents, including hexane/tetrahydrofuran (10:1) for the asymmetric methyl dimer, hexane/tetrahydrofuran (20:1) for the asymmetric ethyl dimer, hexane/ethyl acetate (10:1) for the asymmetric benzylic dimer, and hexane/ethyl acetate (5:1) for the asymmetric aniline dimer. The asymmetric *tert*-butyl dimer was recrystallized three times in hexane. The asymmetric deuterated methyl dimer was prepared by the same method as the asymmetric methyl dimer with the exception of formaldehyde-*d*<sub>2</sub>.

The secondary amines for the asymmetric propyl dimer, asymmetric cyclohexyl dimer, and asymmetric fluoroaniline dimer were prepared before synthesizing the asymmetric dimers. An equimolar solution of benzaldehyde and the appropriate primary amine in hexane was azeotropically distilled until a stoichiometric amount of water had been collected. After evaporating hexane, the resulting crude Schiff base was dissolved in ethanol containing 1 wt % of concentrated ammonium hydroxide and reduced using sodium borohydride.<sup>17</sup> The reaction mixture was diluted with ice water, and the crystalline secondary amine products were collected by filtration. Then, asymmetric propyl dimer, asymmetric cyclohexyl dimer, and asymmetric fluoroaniline dimer were synthesized by the same procedure using these secondary amines. The asymmetric propyl dimer and asymmetric cyclohexyl dimer were purified by column chromatography with silica gel using hexane/tetrahydrofuran (20:1) as eluents. The asymmetric fluoroaniline dimer was recrystallized three times in hexane. The modified asymmetric methyl dimers (Table 4) were also prepared by the same method as above but using different phenols.

**Instrumentation.** The purities of the monomers and dimers were examined using a Varian XL200 nuclear magnetic resonance (NMR) spectrometer (200 MHz <sup>1</sup>H NMR and 50.1

Table 4. Asymmetric Model Dimers II



| Abbreviations                                 | R <sub>1</sub>   | R <sub>2</sub>   | IUPAC chemical names                                 |
|---|------------------|------------------|--|
| <b>4a</b> (Asymmetric Methyl-dimer)           | -CH <sub>3</sub> | -CH <sub>3</sub> | N-benzyl-N-(3,5-dimethyl-2-hydroxybenzyl)methylamine |
| <b>5a</b> (Asymmetric <i>p</i> -Cresol-dimer) | -CH <sub>3</sub> | -H               | N-benzyl-N-(5-methyl-2-hydroxybenzyl)methylamine     |
| <b>5b</b> (Asymmetric <i>p</i> -Fluoro-dimer) | -F               | -H               | N-benzyl-N-(5-fluoro-2-hydroxybenzyl)methylamine     |
| <b>5c</b> (Asymmetric <i>p</i> -Chloro-dimer) | -Cl              | -H               | N-benzyl-N-(5-chloro-2-hydroxybenzyl)methylamine     |
| <b>5d</b> (Asymmetric <i>p</i> -Bromo-dimer)  | -Br              | -H               | N-benzyl-N-(5-bromo-2-hydroxybenzyl)methylamine      |
| <b>5e</b> (Asymmetric 2,4-Fluoro-dimer)       | -F               | -F               | N,N-bis(3,5-difluoro-2-hydroxybenzyl)methylamine     |
| <b>5f</b> (Asymmetric <i>p</i> -Cyano-dimer)  | -CN              | -H               | N-benzyl-N-(5-cyano-2-hydroxybenzyl)methylamine      |
| <b>5g</b> (Asymmetric 2,3-Fluoro-dimer)       | -F*              | -F               | N-benzyl-N-(3,4-difluoro-2-hydroxybenzyl)methylamine |
| <b>5h</b> (Asymmetric <i>p</i> -Nitro-dimer)  | -NO <sub>2</sub> | -H               | N-benzyl-N-(5-nitro-2-hydroxybenzyl)methylamine      |

MHz <sup>13</sup>C NMR at 298 K) using deuterated chloroform as the solvent with 0.5% tetramethylsilane as an internal standard. The coaddition of 64 transients yielded <sup>1</sup>H NMR spectra with good signal-to-noise ratios. A relaxation time (D1) of 10 s was used to obtain integration results. The difference between the values for the actual and calculated C, H, and N content of the models was less than 0.3% (M-H-W Laboratories). The results are summarized in Table 5.

Fourier transform infrared (FT-IR) spectra were obtained using a Bomem Michelson MB110 FT-IR spectrophotometer which was equipped with a liquid nitrogen cooled, mercury–cadmium–telluride (MCT) detector with a specific detectivity, *D*<sup>\*</sup>, of  $1 \times 10^{10}$  cm Hz<sup>1/2</sup> W<sup>-1</sup>. The coaddition of 128 scans was recorded at a resolution of 4 cm<sup>-1</sup> after 20 min purge with nitrogen. FT-IR spectra for polybenzoxazines were obtained from thin films which were cured on potassium bromide (KBr) plates, using the same procedure as in the previous paper.<sup>8</sup>

The solution spectra for the dimers in CCl<sub>4</sub> were obtained in a KRS-5 liquid cell with a 0.5 mm thickness for the 20 and 50 mM concentrations and with a 5 mm thickness for the 1 mM concentration. The spectrum of the liquid cell filled with spectrophotometric grade carbon tetrachloride (CCl<sub>4</sub>) was subtracted from the solution spectra.

Differential scanning calorimetry (DSC) measurements were performed on a TA Instruments 2920 modulated DSC with a heating rate of 10 °C/min under a dry nitrogen atmosphere using the standard mode. The cured polybenzoxazine sample sizes were in the range of 10–15 mg and were analyzed in hermetic aluminum sample pans.

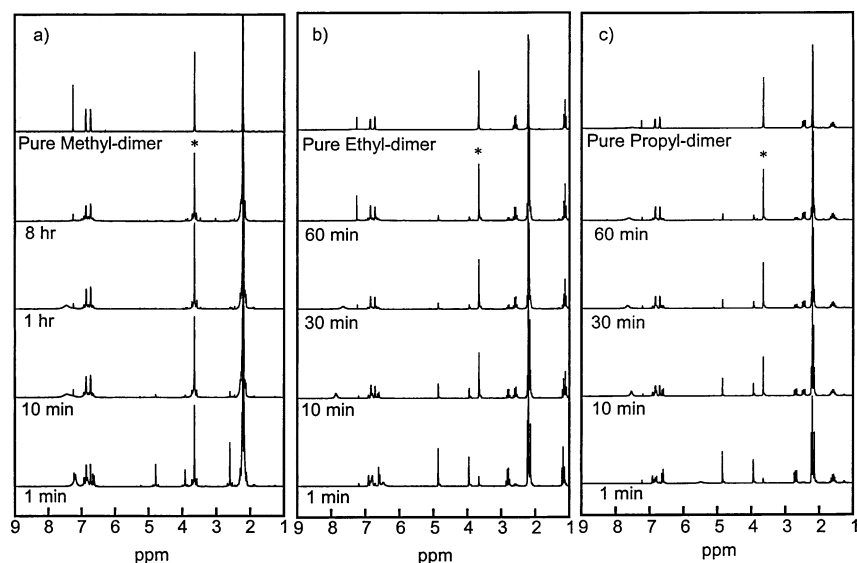
## Results and Discussion

**<sup>1</sup>H NMR Spectra for the Dimerization** According to the previous studies,<sup>6,8,12,13</sup> it is believed that the general polybenzoxazine hydrogen-bonded network structure is affected by the basicity of the amine functional group. Therefore, several aliphatic and aromatic primary amines with different basicities were selected for this study (Table 6). Also, amines having functional groups of differing sizes were chosen in order to evaluate any possible steric effect. If any products (other than the dimer) can be found in the process of dimerization, it is possible that a similar process could occur during the polymer curing reaction. These possible side products are able to alter the hydrogen-bonding scheme of the polymer system, which has been established by the previous study based on pure dimer molecules.

By investigating the <sup>1</sup>H NMR spectra for the conversion from monomer to dimer, the influence of the amine substituents on the dimerization reaction is presently studied. As is shown in Figure 1, the dimerization reactions for the methyl dimer, ethyl dimer, and propyl dimer proceeded without significant side reactions, while the reactions for dimers based on bulkier amines show the signs of many side reactions (Figures 2–4). For the methyl dimer, it is demonstrated that the Mannich base is stable, even after 8 h of continuous reaction, due to the fact that there are no evident signs of side products near the chemical shift for the meth-

Table 5. <sup>1</sup>H NMR Chemical Shift for the Methylene Group in Asymmetric Dimers

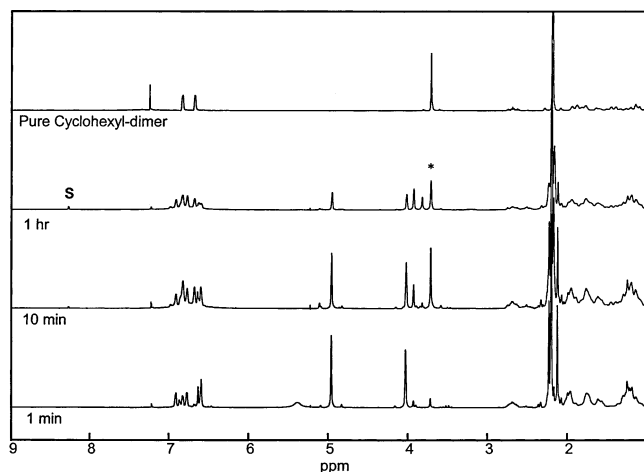
| Materials | Appearance                | Ar-CH <sub>2</sub> -N   |                          | Formula   | Elemental analysis |      |      |           |      |      |
|-----------|---------------------------|-------------------------|--------------------------|---|--------------------|------|------|-----------|------|------|
|           |                           | <sup>1</sup> H-NMR(ppm) | <sup>13</sup> C-NMR(ppm) |   | Calculated (%)     |      |      | Found (%) |      |      |
|           |                           |                         |                          |   | C                  | H    | N    | C         | H    | N    |
| <b>2a</b> | White crystal             | 3.66                    | 59.25                    | C <sub>19</sub> H <sub>25</sub> NO <sub>2</sub>   | 76.22              | 8.42 | 4.68 | 76.40     | 8.54 | 4.60 |
| <b>2b</b> | White crystal             | 3.67                    | 46.52                    | C <sub>20</sub> H <sub>27</sub> NO <sub>2</sub>   | 76.64              | 8.68 | 4.47 | 76.80     | 8.80 | 4.52 |
| <b>2c</b> | White crystal             | 3.66                    | 56.10                    | C <sub>21</sub> H <sub>29</sub> NO <sub>2</sub>   | 77.02              | 8.93 | 4.28 | 76.88     | 9.13 | 4.30 |
| <b>2d</b> | White crystal             | 3.72                    | 51.52                    | C <sub>24</sub> H <sub>33</sub> NO <sub>2</sub>   | 78.43              | 9.05 | 3.81 | 78.57     | 9.03 | 3.76 |
| <b>2e</b> | White needle-like crystal | 4.26                    | 55.68                    | C <sub>24</sub> H <sub>27</sub> NO <sub>2</sub>   | 79.74              | 7.53 | 3.87 | 79.89     | 7.69 | 3.91 |
| <b>3</b>  | White needle-like crystal | 3.84 <sup>(*)</sup>     | 31.14 <sup>(*)</sup>     | C <sub>17</sub> H <sub>20</sub> O <sub>2</sub>    | 79.65              | 7.86 | -    | 80.01     | 7.82 | -    |
| <b>4a</b> | Pale yellow liquid        | 3.593, 3.699            | 61.03, 61.50             | C <sub>17</sub> H <sub>21</sub> NO                | 79.96              | 8.29 | 5.49 | 80.07     | 8.15 | 5.56 |
| <b>4b</b> | Pale yellow liquid        | 3.583                   | 61.49                    | C <sub>17</sub> H <sub>19</sub> D <sub>2</sub> NO | 79.33              | 9.01 | 5.44 | 79.36     | 8.88 | 5.22 |
| <b>4c</b> | Pale yellow liquid        | 3.618, 3.707            | 56.93, 57.52             | C <sub>18</sub> H <sub>23</sub> NO                | 80.26              | 8.61 | 5.20 | 80.38     | 8.63 | 5.30 |
| <b>4d</b> | Pale yellow liquid        | 3.603, 3.698            | 57.65, 58.01             | C <sub>19</sub> H <sub>25</sub> NO                | 80.52              | 8.89 | 4.94 | 80.43     | 8.79 | 5.01 |
| <b>4e</b> | White crystal             | 3.707, 3.865            | 53.34, 54.62             | C <sub>20</sub> H <sub>27</sub> NO                | 80.76              | 9.15 | 4.71 | 80.88     | 9.21 | 4.90 |
| <b>4f</b> | Pale yellow liquid        | 3.628, 3.779            | 52.95, 54.10             | C <sub>22</sub> H <sub>29</sub> NO                | 81.69              | 9.04 | 4.33 | 81.78     | 8.96 | 4.45 |
| <b>4g</b> | White crystal             | 3.573, 3.659            | 57.01, 57.83             | C <sub>23</sub> H <sub>25</sub> NO                | 83.34              | 7.60 | 4.23 | 83.43     | 7.61 | 4.34 |
| <b>4h</b> | Pale yellow liquid        | 4.268, 4.308            | 55.19, 57.68             | C <sub>22</sub> H <sub>23</sub> NO                | 83.24              | 7.30 | 4.41 | 83.49     | 7.12 | 4.63 |
| <b>4i</b> | White crystal             | 4.164, 4.199            | 56.06, 57.14             | C <sub>22</sub> H <sub>22</sub> FNO               | 78.78              | 6.61 | 4.18 | 78.60     | 6.72 | 4.28 |
| <b>5a</b> | White crystal             | 3.600, 3.720            |                          |   |                    |      |      |           |      |      |
| <b>5b</b> | White crystal             | 3.605, 3.712            |                          |   |                    |      |      |           |      |      |
| <b>5c</b> | White crystal             | 3.615, 3.721            |                          |   |                    |      |      |           |      |      |
| <b>5d</b> | White crystal             | 3.596, 3.707            |                          |   |                    |      |      |           |      |      |
| <b>5e</b> | Pale yellow liquid        | 3.628, 3.755            |                          |   |                    |      |      |           |      |      |
| <b>5f</b> | White crystal             | 3.627, 3.768            |                          |   |                    |      |      |           |      |      |
| <b>5g</b> | Pale yellow liquid        | 3.628, 3.769            |                          |   |                    |      |      |           |      |      |
| <b>5h</b> | Light yellow crystal      | 3.694, 3.862            |                          |   |                    |      |      |           |      |      |



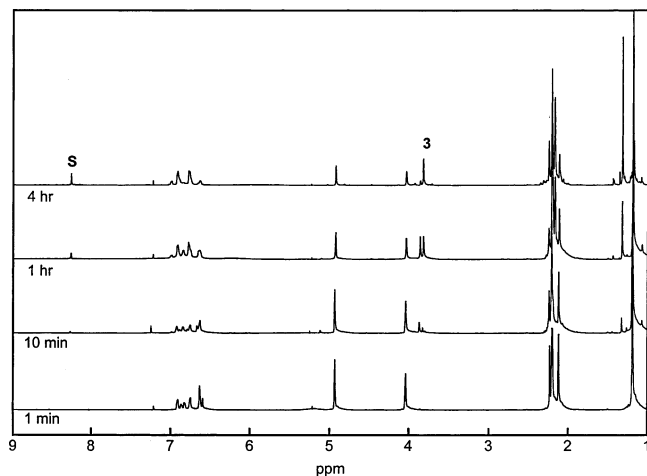
**Figure 1.**  $^1\text{H}$  NMR spectra of model dimers at 155  $^{\circ}\text{C}$ : (a) methyl dimer, (b) ethyl dimer, and (c) propyl dimer.

**Table 6.**  $\text{p}K_{\text{a}}$  of Primary Amines and Phenols<sup>18</sup>

| compd   |                                  | $\text{p}K_{\text{a}}$ |
|---------|----------------------------------|------------------------|
| amines  | methylamine                      | 10.66                  |
|         | ethylamine                       | 10.71                  |
|         | <i>n</i> -propylamine            | 10.61                  |
|         | <i>n</i> -butylamine             | 10.64                  |
|         | <i>tert</i> -butylamine          | 10.69                  |
|         | cyclohexylamine                  | 10.69                  |
|         | benzylamine                      | 9.30                   |
| phenols | aniline                          | 4.63                   |
|         | <i>o</i> -fluoroaniline          | 3.20                   |
|         | 2,4-dimethylphenol               | 10.58                  |
|         | <i>p</i> -cresol                 | 10.26                  |
|         | <i>p</i> -fluorophenol           | 9.89                   |
|         | <i>p</i> -chlorophenol           | 9.43                   |
|         | <i>p</i> -bromophenol            | 9.34                   |
|         | 2,4-difluorophenol <sup>19</sup> | 8.40                   |
|         | <i>p</i> -cyanophenol            | 7.80                   |
|         | 2,3-difluorophenol <sup>19</sup> | 7.68                   |
|         | <i>p</i> -nitrophenol            | 7.15                   |

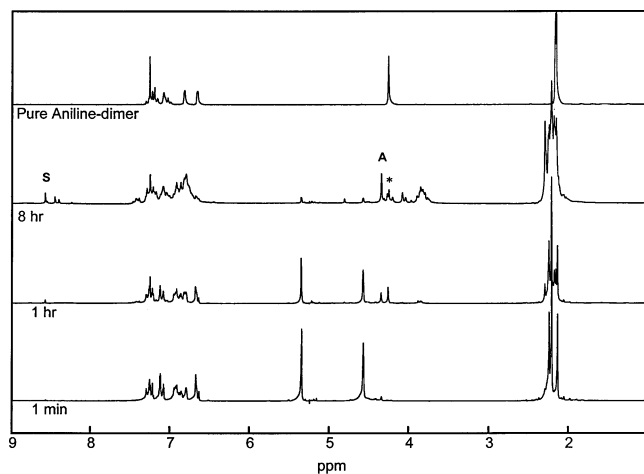


**Figure 3.**  $^1\text{H}$  NMR spectra of cyclohexyl dimer at 155  $^{\circ}\text{C}$ .



**Figure 2.**  $^1\text{H}$  NMR spectra of *tert*-butyl dimer at 155  $^{\circ}\text{C}$ .

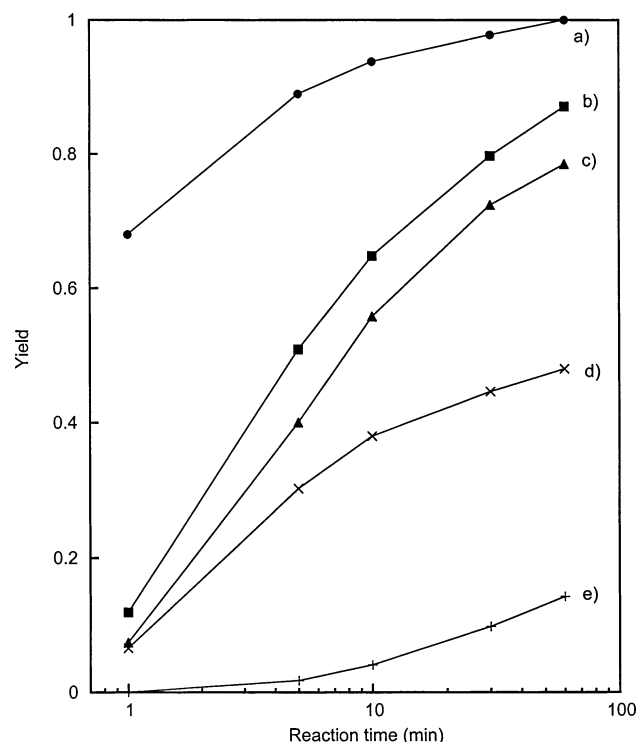
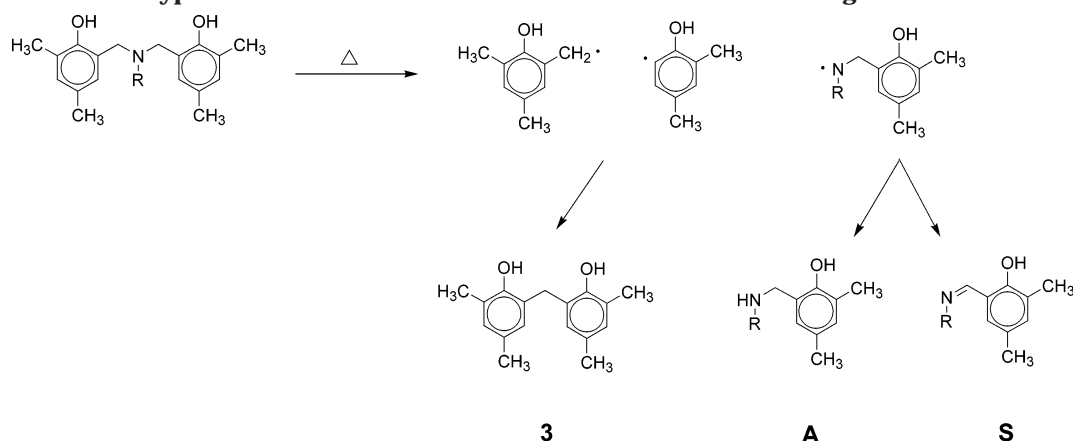
ylene proton (\* marked) of the dimer. Although the conversion to the dimer calculated from the integral of the methylene proton resonance in  $^1\text{H}$  NMR is slowed as is shown in Figure 5, the ethyl dimer and propyl dimer have similar  $^1\text{H}$  NMR spectra to the methyl dimer. This result suggests that the dimers based on methylamine, ethylamine, and propylamine can well simulate the polymer.



**Figure 4.**  $^1\text{H}$  NMR spectra of aniline dimer at 155  $^{\circ}\text{C}$ .

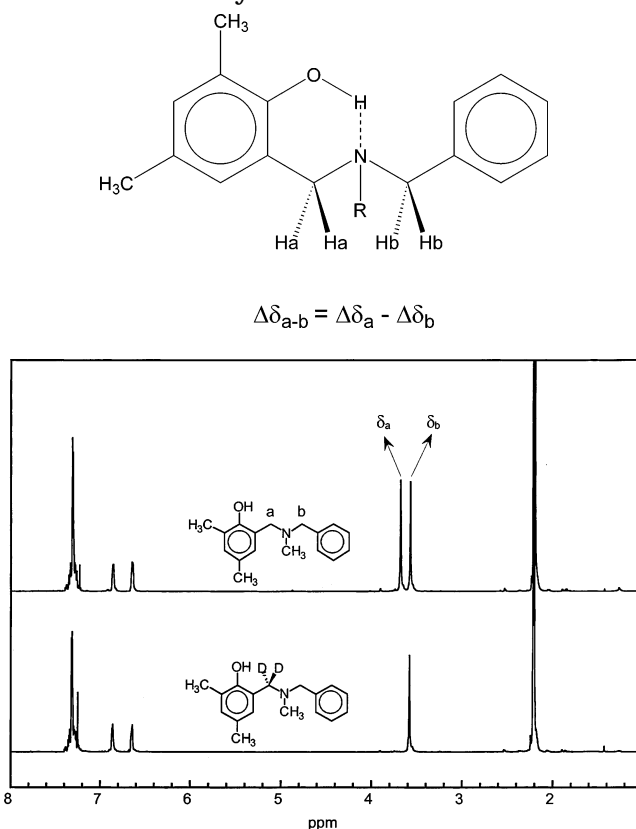
On the other hand, the reaction of the *tert*-butyl dimer is very different and shows no stable dimer formation (Figure 2). Since a detailed study of the ring-opening mechanism of benzoxazine monomers is beyond the scope of this paper, the complete separation of all reaction products was not attempted. However, some of the important products were successfully separated (**S**, **A**, and **3** in Figures 2, 3, and 4) by recrystallization.



**Scheme 3. Typical Side Products of Dimerization and Possible Cleavage of Mannich Base****Figure 5.** Yield of symmetric dimers: (a) methyl dimer, (b) ethyl dimer, (c) propyl dimer, (d) cyclohexyl dimer, and (e) aniline dimer.

Especially, major formation of phenolic dimer, rather than the *tert*-butyl dimer, implies that the dimer formation is greatly influenced by the structure of substituted amine functional group. This methylene bridge formation involving an early degradation process of the Mannich bridge has been investigated in detail by Low and Ishida<sup>20,21</sup> (Scheme 3). A similar observation is found in the dimer formation process for the dimers based on bulky amines, cyclohexylamine and aniline, and it can be supported by the fact that the percentage yield of dimers based on bulky amines is drastically decreased with increasing amine size.

**Effect of Amine Substituents on  $-\text{OH}\cdots\text{N}$  Intramolecular Hydrogen Bonding.** Since the asymmetric dimers simulate well the nature of  $-\text{OH}\cdots\text{N}$  intramolecular hydrogen bonding,<sup>13</sup> the difference in intramolecular hydrogen bonding between the asymmetric dimers is evaluated by  $^1\text{H}$  NMR. The  $-\text{OH}\cdots\text{N}$  intramolecular hydrogen bonding forms a stable six-membered structure,<sup>13</sup> resulting in a methylene proton

**Scheme 4. Deshielding Effect in  $^1\text{H}$  NMR Due to  $-\text{OH}\cdots\text{N}$  Intramolecular Hydrogen Bonding in Asymmetric Dimers****Figure 6.** Chemical shift differences for methylene protons in the asymmetric dimer.

deshielding effect in methylene protons (Scheme 4). As is shown in Figure 6, the methylene protons in asymmetric dimers have different chemical shifts due to the deshielding effect. From the  $^1\text{H}$  NMR spectra for the asymmetric deuterated methyl dimer (which does not have  $\delta_a$ ), it can be concluded that the resonances of deshielded protons appear downfield. If the asymmetric dimer structure is identical, aside from the amine functional groups, the effect of the amine substituents on the  $-\text{OH}\cdots\text{N}$  intramolecular hydrogen bonding can be determined by evaluating the chemical shift difference between the two kinds of methylene protons ( $\Delta\delta_{a-b}$ ). As is shown in Figure 7, the asymmetric dimers made with less basic aromatic amines have fewer pronounced differences in chemical shift as compared

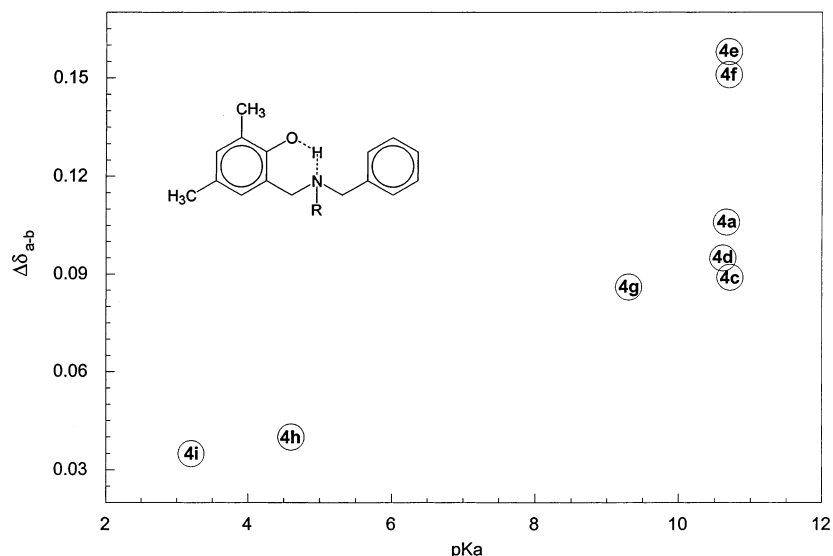


**Figure 7.** Dependence of chemical shift differences for methylene protons in asymmetric dimers based upon the basicities of primary amines.

to the asymmetric dimers based on more basic aliphatic amines. Even if the aromatic shielding effect of the aniline ring is considered, the absolute difference between the two methylene groups is obvious regardless of the aromaticity of substituents. A similar discussion has been reported by Ma and Warnhoff<sup>22</sup> that the downfield N-methyl shift due to protonation in aromatic amine is relatively smaller than that of aliphatic amine. This effect is closely related to the effective negative charge on the nitrogen atom. Considering that the formation of OH $\cdots$ N intramolecular hydrogen bonding in asymmetric dimers is closely related in the electronegativity of the –OH and –N group, it can be predicted that the basicity of amine functional group has a great influence on the formation of an intramolecular hydrogen bond.

However, it is shown that the chemical shift difference is widely spread between the dimers based on aliphatic amines even with the very similar pK<sub>a</sub>. A pair of dimers **4c** and **4g**, based on aliphatic amines with different pK<sub>a</sub>, have similar Δδ<sub>a-b</sub>. The same is observed in another pair of **4a/4g** and **4d/4g**. The interesting point here is that four amines used for the preparation of asymmetric dimers have similar structure with a general formula NH<sub>2</sub>–CH<sub>2</sub>–R, where R = H for **4a**, R = CH<sub>3</sub> for **4c**, R = CH<sub>2</sub>CH<sub>3</sub> for **4d**, and R = C<sub>6</sub>H<sub>5</sub> for **4g**. Although these amines have different overall size, they all have a methylene group that separates their amino group from the substituent R. The substituent R is located rather far from the hydrogen bond; thus, it does not have major influence on the conformation of the OH $\cdots$ N intramolecular hydrogen bonding. In contrast, the asymmetric dimers based on bulky amines show higher Δδ<sub>a-b</sub> values despite their similar basicities. Since cyclohexylamine and *tert*-butylamine do not have a methylene group between the amino group and the substituent, the substituent size plays a profound effect on the hydrogen bonding and Δδ<sub>a-b</sub> of their asymmetric dimers. This means that the structural change near the nitrogen atom plays an importance role in addition to the basicity effect.

To exclude the structural effect of amine substituents, a new series of asymmetric dimers which have the same methylamine group for each dimer were prepared using

different phenols with different pK<sub>a</sub>'s (Table 6). Since N-substituents are all the same for this series of asymmetric dimers, the effect of acidity of the –OH group on the –OH $\cdots$ N intramolecular hydrogen bonding can be investigated without the interference of the steric effect. As is shown in Figure 8, it is clearly seen that the Δδ<sub>a-b</sub> increases with increased phenolic acidity. This good correlation between the acidity of phenols and Δδ<sub>a-b</sub> implies that the larger the chemical shift difference between methylene groups is, the more stable the OH $\cdots$ N intramolecular hydrogen bonding.

**FT-IR Study of Model Dimers.** The FT-IR spectra of the symmetric model dimers were obtained in order to study the basic nature of hydrogen bonding due to changes in the amine substituents, as shown in Figure 9. Using the result from a previous study,<sup>13</sup> the stretching frequencies for hydrogen-bonded hydroxyl groups are investigated in detail. No significant differences in the FT-IR spectra can be found between the linear aliphatic amine-based dimers and their bulkier aliphatic amine-based dimer counterparts of similar basicities. This is somewhat unexpected, considering that the Δδ<sub>a-b</sub> in asymmetric dimers is related in the bulkiness of the substituents. This implies that the effect of the structural bulkiness, which is shown in <sup>1</sup>H NMR of the methylene protons, on the fundamental hydrogen-bonding scheme is not noticeable in the FT-IR spectra. On the other hand, the spectrum of the aniline dimer shows a clear difference in the hydrogen-bonded structure due to the significantly lower basicity of the aniline, as expected. This implies that the dimers based on amines of similar basicities show the similar hydrogen-bonding scheme, regardless of the bulkiness of the functional group.

However, it is apparent in Figure 9 that the intensity of the band centered at 3550 cm<sup>–1</sup>, which is assigned to –OH $\cdots$ π intramolecular hydrogen bonding,<sup>13</sup> increases with increasing amine size. Although a quantitative comparison for this band cannot be given because of the differences in the specific absorptivities for each hydrogen-bonded species, a qualitative analysis can be made by the comparison of this band to the other bands. Since the –OH $\cdots$ π intramolecular hydrogen bonding is influenced by the conformational structure,<sup>23</sup> the increase

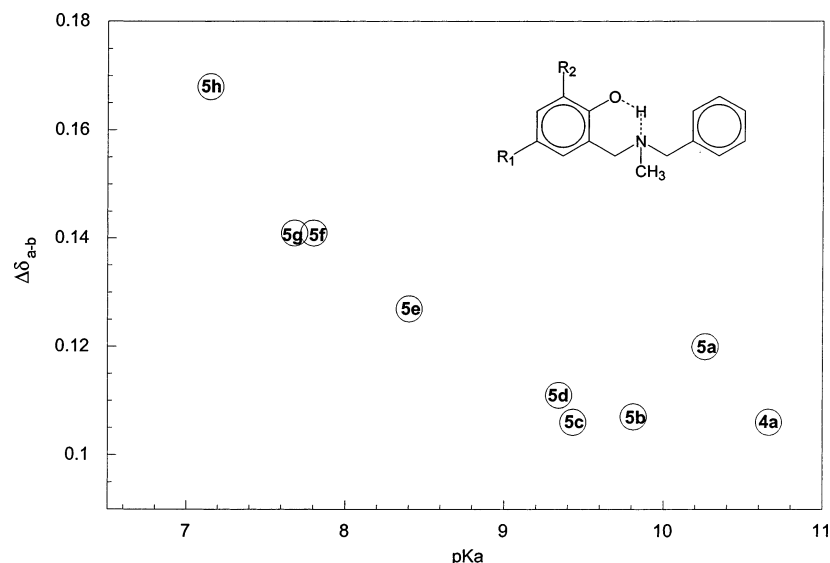


**Figure 8.** Dependence of chemical shift differences for methylene protons in asymmetric dimers based upon the acidities of phenols.

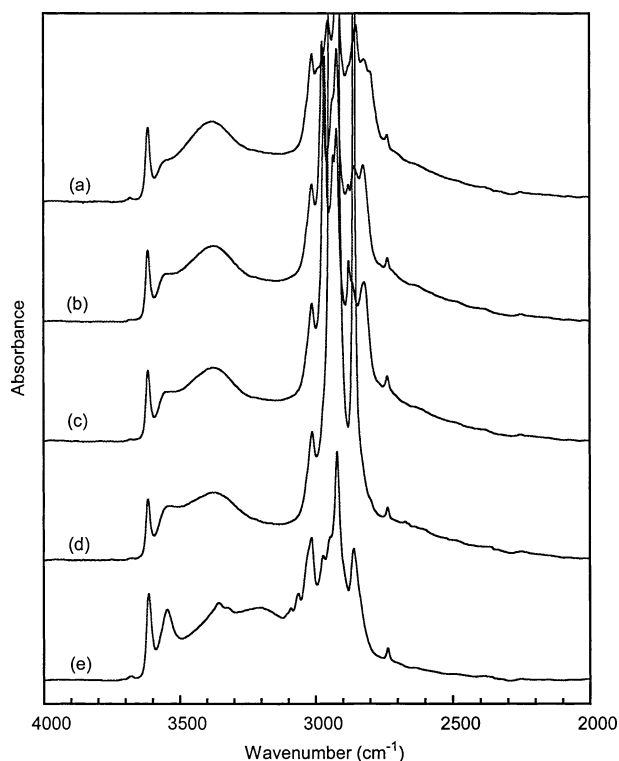


**Figure 9.** FTIR spectra in the region of the hydroxyl stretching frequency for symmetric dimers in CCl<sub>4</sub> (50 mM) solution: (a) methyl dimer, (b) ethyl dimer, (c) propyl dimer, (d) cyclohexyl dimer, and (e) aniline dimer.

in the 3550 cm<sup>-1</sup> band suggests that the change in the larger amine substituents causes a conformational change in which the preferential structure may form –OH... $\pi$  intramolecular hydrogen bonding. This can be seen more readily in the spectra of the asymmetric dimers in CCl<sub>4</sub> where OH...O intramolecular hydrogen bonding has been intentionally removed from the dimer structure (Figure 10).

**Polybenzoxazines.** To investigate hydrogen bonding in polybenzoxazines, the FT-IR spectra of a number of polybenzoxazines were obtained and are shown in Figure 11. Polybenzoxazines based on linear aliphatic amines, the BA-m, BA-e, BA-p, and BA-nb polymers,

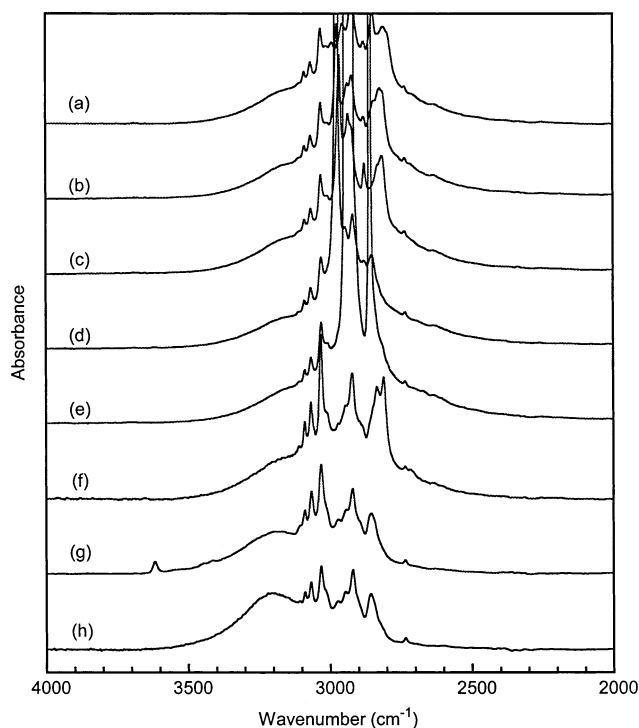


**Figure 10.** FTIR spectra in the region of the hydroxyl stretching frequency for asymmetric dimers in CCl<sub>4</sub> (50 mM) solution: (a) asymmetric methyl dimer, (b) asymmetric ethyl dimer, (c) asymmetric propyl dimer, (d) asymmetric *tert*-butyl dimer, (e) asymmetric cyclohexyl dimer, (f) asymmetric benzyl dimer, (g) asymmetric aniline dimer, and (h) asymmetric fluoroaniline dimer.

have similar hydrogen-bonding schemes. And, using the group frequencies for the hydrogen-bonding species in corresponding model dimers,<sup>13</sup> it is found that the hydrogen-bonding schemes in linear aliphatic amine-based polybenzoxazines are mainly comprised of –OH...N intramolecular hydrogen-bonding interactions which appear as a broad band from 2700 to 3300 cm<sup>-1</sup> in the FT-IR spectra. It has been reported that this stable –OH...N intramolecular hydrogen bonding is attributed to the basicity of methylamine based upon the FT-IR spectra of model benzoxazine methyl dimers.<sup>13</sup> It seems that this explanation applies well to some other linear

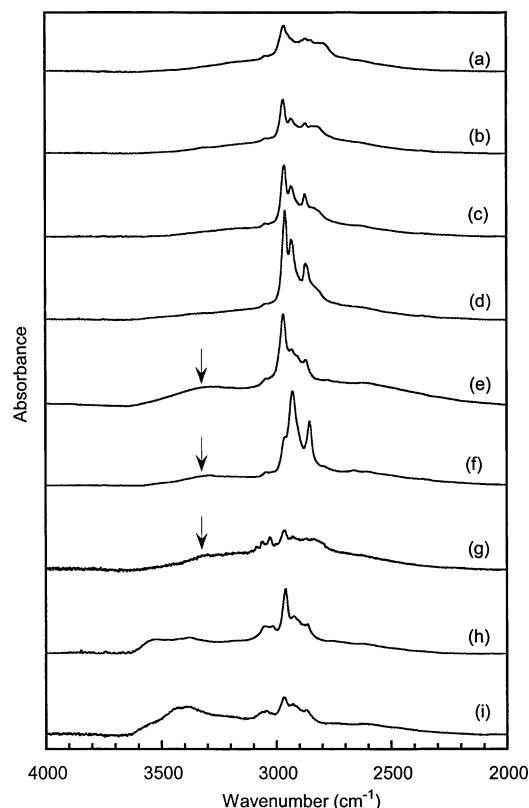


**Figure 11.** FTIR spectra for polybenzoxazines in the region of hydroxyl stretching frequency: (a) BA-m polymer, (b) BA-e polymer, (c) BA-p polymer, (d) BA-nb polymer, (e) BA-tb polymer, (f) BA-c polymer, (g) BA-Bz polymer, (h) BA-a polymer, and (i) BA-fa polymer.

aliphatic amine-based polybenzoxazines, as is shown in Figure 1a–d. In contrast, two polybenzoxazines based on aromatic amines, the BA-a and BA-fa polymers, have been found to contain significant amounts of intermolecular hydrogen bonding ( $3400\text{ cm}^{-1}$ ) while the intramolecular hydrogen-bonding interaction ( $3550\text{ cm}^{-1}$ ) is relatively weak. An appropriate explanation is that the change in the electronegativity of the nitrogen atom, due to the nature of particular amine substituents, is responsible for this difference.

Despite the similar basicities of the corresponding primary amines, the bulkier aliphatic amine-based polybenzoxazines, the BA-tb, BA-c, and BA-Bz polymers, have an obviously different hydroxyl stretching band around  $3350\text{ cm}^{-1}$  which is indicative of the existence of different hydrogen-bonding species. Furthermore, it should be noted that the BA-nb and BA-tb polymer spectra exhibit large differences in this region because of conformational differences in the molecules, despite having amines of the same basicity. Considering the FT-IR spectra for the dimers based on aliphatic amines show a similar hydrogen-bonding scheme, this unexpected difference in FT-IR spectra for the bulkier amine-based polybenzoxazines implies that the hydrogen-bonded structure in polybenzoxazines cannot be deduced simply on the basis of the basicities of corresponding amines alone. It is possible that a structural factor, in addition to the basicity of the primary amine, may strongly affect the hydrogen-bonded network structure of the polymer.

It is logically deduced that side reactions during dimerization, including Schiff base and phenolic methylene bridge formation, can occur during the polymerization of the corresponding BA-tb, BA-c, and BA-Bz polymers, resulting in the observed differences in the polymer FT-IR spectra. Also of great importance, the spectra of the phenolic dimer give insight into the origin of the band at  $3350\text{ cm}^{-1}$  in the spectra of the BA-tb, BA-c, and BA-Bz polymers. As is shown in Figure 12, the broad band around  $3350\text{ cm}^{-1}$  for the phenolic dimer in  $20\text{ mM CCl}_4$  solution is due to the  $-\text{OH}\cdots\text{O}$  intermolecular hydrogen bonding as this band does not appear in the spectrum of the dilute solution at  $1\text{ mM}$ . Taking into account that the  $-\text{OH}\cdots\text{O}$  intermolecular hydrogen bonding in the symmetric methyl dimer<sup>13</sup> is assigned to the band at  $3401\text{ cm}^{-1}$ , it can be concluded that the band at  $3350\text{ cm}^{-1}$  in the BA-tb, BA-c, and BA-Bz polymers originates from the methylene bridge structure which is formed during the thermal curing of the monomer.

It is also shown in Figure 13 that this aspect of the dimerization process affects the polymerized network structure. Since typical bifunctional benzoxazine monomer is polymerized and cross-linked upon curing, solu-

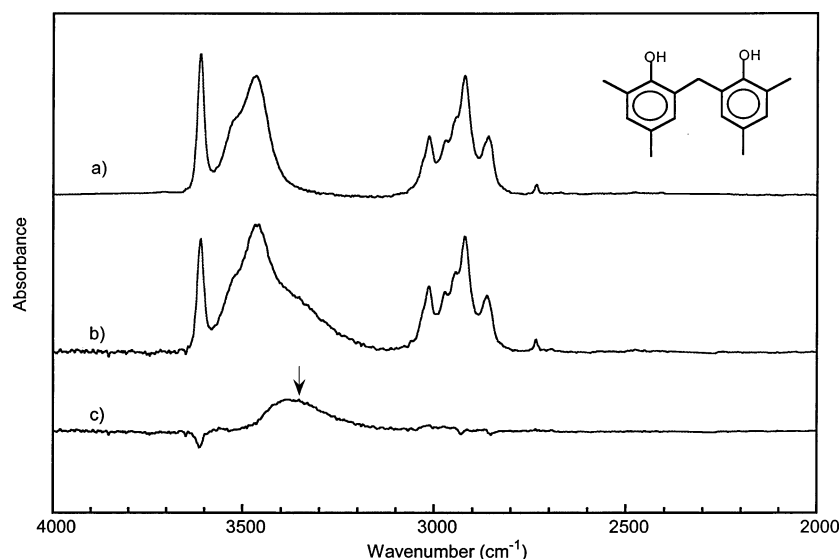


**Figure 12.** FT-IR spectra for phenolic dimer in  $\text{CCl}_4$  solution: (a)  $1\text{ mM}$  concentration, (b)  $20\text{ mM}$ , and (c) subtracted spectrum (b) – (c).



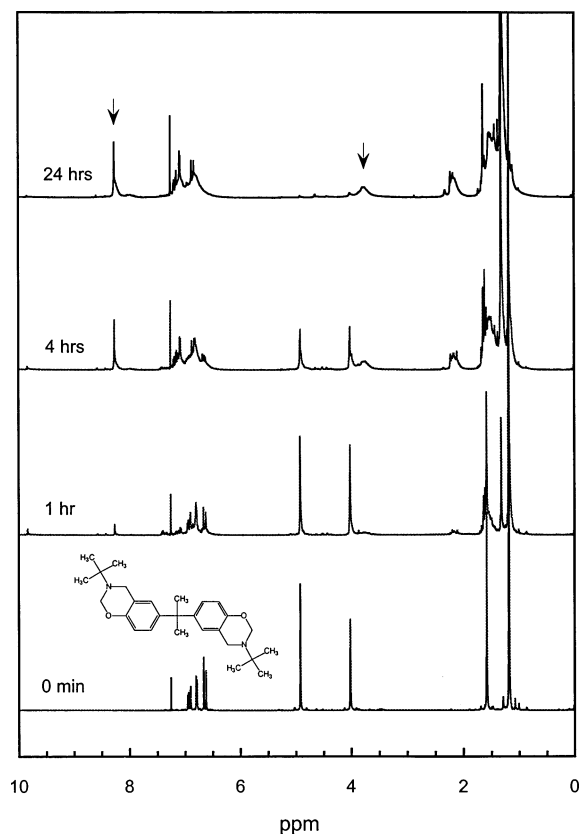


**Figure 13.**  $^1\text{H}$  NMR spectra of curing profile for BA-tb monomer at 155  $^{\circ}\text{C}$ .

tion  $^1\text{H}$  NMR spectra cannot be obtained due to insolubility in the NMR solvents. However, since the polymerized product of the BA-tb monomer is unexpectedly soluble in deuterated chloroform even after complete disappearance of the monomer,  $^1\text{H}$  NMR spectra can be obtained. This solubility of the product indicates that the network structure of the polymer is not formed. Instead, resonances appeared that correspond to a Schiff base (8.2 ppm) and phenolic oligomer (3.6 ppm), which are possible degradation products of the Mannich base. This implies that the hydrogen-bonded network structure in bulkier amine-based polybenzoxazines is affected by the hydrogen-bonded species, not only around the Mannich base but also in phenolic linkages.

It is shown in Figure 14 that the structural differences between amines with similar basicities have an influence on the glass transition temperature ( $T_g$ ) of polybenzoxazines. Taking into account that the  $T_g$  of a thermoset polymer is closely related to polymer chain mobility and packing, the present effect on the  $T_g$  of the polymer might be explained by the structural effect of the amine substituents which has been reported by Ishida and Low.<sup>6</sup> Also, it has been reported that the relatively high  $T_g$  of the BA-a polymer, which has a significantly bulky substituent, is attributed to a secondary reaction of the ortho position of phenyl substituent<sup>20,24</sup> along with the tight packing of the polymer chains due to strong hydrogen bonding,<sup>6,8</sup> in addition to the primary network structure connected by the Mannich bridge. However, from the results of this study, it is shown that the formation of an effective cross-linked structure is interfered with by the extensive degradation process during polymerization for the bulkier amine-based polybenzoxazines without secondary reaction site,

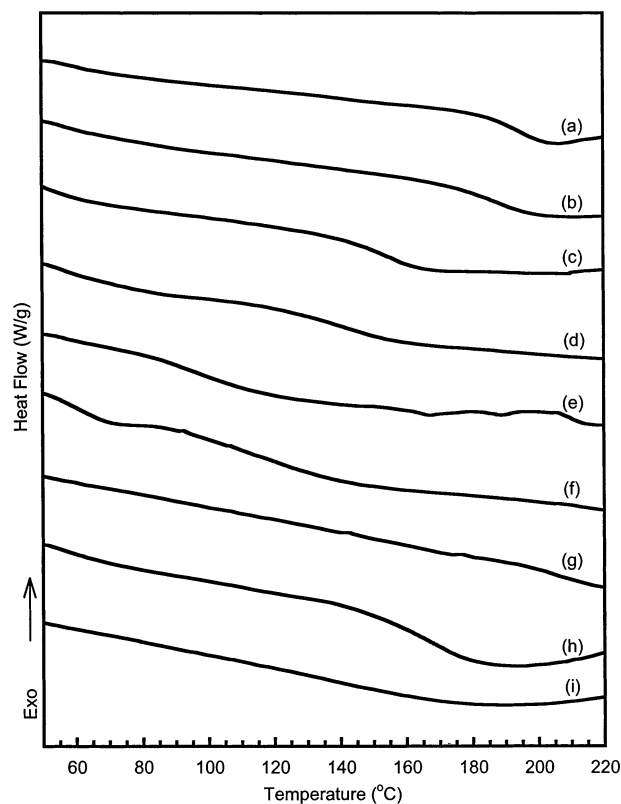


**Figure 14.** Glass transition temperature ( $T_g$ ) in the DSC thermograms for polybenzoxazines: (a) BA-m polymer, (b) BA-e polymer, (c) BA-p polymer, (d) BA-nb polymer, (e) BA-tb polymer, (f) BA-c polymer, (g) BA-Bz polymer, (h) BA-a polymer, and (i) BA-fa polymer.

in addition to the steric effect, resulting in a lowered  $T_g$ .

## Conclusions

Hydrogen bonding in polybenzoxazines has been investigated utilizing the FT-IR and  $^1\text{H}$  NMR spectra of model dimers having various molecular sizes and basicities. The ability to investigate  $-\text{OH}\cdots\text{N}$  intramolecular hydrogen bonding has been demonstrated through the analysis of the magnetic nonequivalence of the methylene protons in the Mannich base of asymmetric dimer compounds. From comparisons of the FT-IR spectra of polybenzoxazines and model dimers, it has been shown that if the amine constituents have similar basicities, the nature of hydrogen bonding is very similar. The steric aspect of bulkier amines has a more profound effect on the stability of the Mannich base, resulting in heterogeneous products during the ring-opening reaction. It has also been demonstrated that bifunctional benzoxazine monomers based on extremely bulky amines, such as that in the BA-tb monomer, cannot form completely cross-linked polymer networks due to the extensive degradation process.

## References and Notes

- (1) Sijbesma, R. P.; Beijer, F. H.; Brunsveld, L.; Folmer, B. J. B.; Hirschberg, J. H. K. K.; Lange, R. F. M.; Lowe, J. K. L.; Meijer, E. W. *Science* **1997**, *278*, 1601.
- (2) Brunet, P.; Simard, M.; Wuest, J. D. *J. Am. Chem. Soc.* **1997**, *119*, 2737.
- (3) Castellano, R. K.; Rebek, J., Jr. *J. Am. Chem. Soc.* **1998**, *120*, 3657.
- (4) Ishida, H.; Allen, D. J. *J. Polym. Sci., Polym. Phys.* **1996**, *34*, 1019.

- (5) Shen, S. B.; Ishida, H. *Polym. Comput.* **1996**, *17*, 710.
- (6) Ishida, H.; Low, H. Y. *Macromolecules* **1997**, *30*, 1099.
- (7) Ning, X.; Ishida, H. *J. Polym. Sci., Polym. Chem. Ed.* **1994**, *32*, 1121.
- (8) Kim, H. D.; Ishida, H. *J. Appl. Polym. Sci.* **2001**, *79*, 1207.
- (9) Macko, J.; Ishida, H. *J. Polym. Sci., Polym. Phys.* **2000**, *38*, 2687.
- (10) Ishida, H.; Rodriguez, Y. *Polymer* **1995**, *36*, 3151.
- (11) Wirasate, S.; Dhumrongvaraporn, S.; Allen, D. J.; Ishida, H. *J. Appl. Polym. Sci.* **1998**, *70*, 1299.
- (12) Dunkers, J. P.; Zarate, A.; Ishida, H. *J. Phys. Chem.* **1996**, *100*, 13514.
- (13) Kim, H. D.; Ishida, H. *J. Phys. Chem. A* **2002**, *106*, 3271.
- (14) Goward, G. R.; Schnell, I.; Brown, S. P.; Spiess, H. W.; Kim, H. D.; Ishida, H. *Magn. Reson. Chem.* **2001**, *39*, S5.
- (15) Ishida, H. US Pat. 5,543,516, Aug 6, 1996.
- (16) Dunkers, J.; Ishida, H. *Spectrochim. Acta* **1995**, *51A*, 855.
- (17) Derieg, M. E.; Sternbach, L. H. *J. Org. Chem.* **1966**, June, 237.
- (18) Dean, J. A. *Lange's Handbook of Chemistry*; McGraw-Hill: New York, 1972; pp 8–20.
- (19) Stefanidis, D.; Cho, S.; Dhe-Paganon, S.; Jencks, W. P. *J. Am. Chem. Soc.* **1993**, *115*, 1650.
- (20) Low, H. Y.; Ishida, H. *J. Polym. Sci., Polym. Phys.* **1998**, *36*, 1935.
- (21) Low, H. Y.; Ishida, H. *Polymer* **1999**, *40*, 4365.
- (22) Ma, J. C. N.; Warnhoff, E. W. *Can. J. Chem.* **1965**, *43*, 1849.
- (23) Cairns, T.; Eglinton, G. *J. Chem. Soc.* **1965**, 5906.
- (24) Ishida, H.; Sanders, D. P. *Polymer* **2001**, *42*, 3115.

MA030108+